Hindawi
Journal of Chemistry
Volume 2021, Article ID 7405238, 16 pages
https://doi.org/10.1155/2021/7405238

*Research Article*

# Effective Approach of Activated Jordanian Bentonite by Sodium Ions for Total Phenolic Compounds Removal from Olive Mill Wastewater

**Khansaa Al-Essa** [1] **and Ethar M. Al-Essa** [2]

[1]*Department of Chemistry, Jerash University, Jerash 26150, Jordan*
[2]*Department of Civil Engineering, University of Canterbury, Christchurch, New Zealand*

Correspondence should be addressed to Khansaa Al-Essa; khansaa.essa@gmail.com

Received 16 April 2021; Accepted 18 June 2021; Published 7 July 2021

Academic Editor: Shayessteh Dadfarnia



Olive mill wastewater (OMW) is nowadays considered a serious environmental problem, especially within the Mediterranean region. With this in mind, water shortages are also a very serious and prevalent concern in third world countries. The aim of this study is to investigate the feasibility of using Jordanian bentonite, a simple and natural clay, as a possible adsorbent to decrease the negative characteristics of raw OMW, as an approach to the development of a methodology that addresses the OMW problem without affecting freshwater resources. The purified bentonite was activated by sodium ions at room temperature. FTIR, XRD, TGA, and BET surface area measurements were performed. OMW was contacted with both purified and activated bentonite in the batch technique to figure out the optimum parameters for the adsorption process. Physiochemical parameters of OMW were measured before and after treatment. The maximum adsorption $q_m$ was found as 8.81 mg/g at 323 K for the total phenolic compounds. The Langmuir and Freundlich models were utilized to describe the equilibrium isotherms and both models fit well. The parameters of thermodynamic show that the adsorption process was feasible, spontaneous, and endothermic in nature. These promising results along with the sodium activation of bentonite significantly improve bentonite's adsorption capacity.

## 1. Introduction

Bentonite can potentially be utilized as an effective adsorbent towards wastewater treatment due to its low cost and eco-friendly properties. Primarily, this is due to bentonite's high surface area and chemical stability. Bentonite, after some modifications, displayed greater stability in comparison to other minerals studied in relation to the adsorption/desorption process [1]. Enhancing the adsorption capacity of bentonite achieved by different activation methods which include acid activation [2, 3], organic activation [4, 5], nanobentonite composite [6, 7], polymer, and surfactant bentonite composite [8, 9], along with the combinations of bentonite-zeolite with bentonite-alum and bentonite-limestone [10] was examined. Bentonite is one of the most desirable adsorbents for the removal of several pollutants from wastewater [6]. Some researchers have also recommended the use of bentonite as an adsorbent for removing organic compounds [11, 12], oil content [13], and inorganic pollutants (such as heavy metal ions) [14–17], in addition to drug components [18, 19]. However, it was noted in the literature that treatment of olive mill wastewater (OMW) with a low-cost modified bentonite as being poorly discussed [20] and that more studies are needed. Jordanian Bentonite has significant physical, chemical, nontoxicity, and unique adsorption properties, along with its high specific surface area and cation exchange capacity (53–85 mEq/100 g) [21]. Some studies focused on the adsorption capacity of Jordanian bentonite toward some heavy metal ions, such as Ni(II), Co(II) [22], Th(IV), U(VI) [23], and Pb(II) [24], but the activation of Jordanian bentonite and its adsorption capacity for removing pollutants from OMW has not been studied in

detail. Therefore, an adsorption isotherms study of total phenolic compounds (TPC) removal, along with the effects of different parameters on adsorption efficiency, needs to be conducted. Phenolic compounds have attracted great interest, with them being widely utilized in industrial processes to obtain petrochemical products, dyes, rubber, plastics, textiles, paper, foams, emulsifiers, and detergents [25]. They are also produced by different industries such as the drug industry and the olive oil production [26]. These compounds have been extensively discharged into wastewaters [27]. Such wastewater containing these kinds of pollutants is of concern due to its potential severe hazard and threat to human health, aquatic life, and groundwater [28]. Some of the phenolic compounds have high toxicity and nonbiodegradable substances and are persistent in the environment [29]. Dangerously, conventional biological processes do not have the ability to remove all phenolic contaminants that are present in industrial wastewater. The structures of the eleven phenols considered priority pollutants by the US Environmental Protection Agency (EPA) are shown in Figure 1. These highly toxic compounds for both humans and the environment as a whole may cause inflammation in the digestive system, an increase in blood pressure, and a reduction of blood ability to carry oxygen to tissues and organs [30, 31]. Hence, phenolic compounds should be removed entirely from wastewater before being discharged into the environment [32].

Adsorption technology in particular has been utilized for the removal of organic compounds from wastewater [33]. Olive oil is an important industry sector, being the main component of the Mediterranean food [34]. Its seasonal production is accompanied with large quantities of OMW in a relatively short period. OMW is a dangerous environmental problem, with its high pollutant load, high turbidity, low pH, high salinity, and high organic content including phenolic compounds, organic acids, and polysaccharides, which are nonbiodegradable. OMW's observable consequence includes the discoloring of both surface and groundwater, as well as affecting the soil quality and harming plant and aquatic organisms [35].

Mediterranean countries, specifically Jordan, face a serious problem in managing OMW. OMW is mostly generated from small mills with outdated technologies for oil extraction. These mills usually have limited financial resources and are located far from each other. Due to their location, it is difficult to establish a central treatment location with the disposal facilities. Ergo, there is a need for effective technologies suitable for small scale olive mills that can decrease the environmental impact of OMW. Some methods have been implemented to treat OMW with varying degrees of success [36], eventhough a major drawback concerning some techniques is their high capital cost and low toxicity reduction. To manage the OMW sustainably, continuous research on the application of Jordanian bentonite has been conducted [1, 2]. Further activation methods will be introduced as an alternative low cost and environmentally safe adsorbent. The activated Jordanian bentonite (AJB) may offer the ability to reutilize OMW for irrigation and industrial purposes as a sustainable approach to reduce the odor and contamination of soil, surface, and groundwater.

In this study, OMW collected from different olive oil mills in Jerash city will be characterized. The Jordanian Ca-bentonite is activated by sodium ions to produce an efficient adsorbent with improved adsorption capacity toward pollutants in OMW. AJB will be examined as an adsorbent for the removal of TPC from OMW, investigated for the effect of the adsorbent dosage as well as the initial concentration and temperature on adsorption efficiency. AJB will also be examined to establish the adsorption isotherms and simulate the experimental data with the Langmuir and Freundlich adsorption models and estimate the thermodynamic parameters of the TPC adsorption onto AJB adsorbent.

It is hoped that the findings of this study cover the information gap missing from the existing scientific literature concerning sodium AJB and OMW treatment.

## 2. Materials and Methods

The natural Jordanian Ca-Bentonite clay used in this study was collected from the airport region, Al Azraq. The sample was crushed to particle size >250 $\mu$m using a ball mill instrument. All chemicals used are of analytical grade.

*2.1. Purification of Raw Bentonite.* The purification steps were followed in detail as mentioned in the previous study [1]. The raw bentonite sample was dispersed in distilled water at 22°C, and the clay fraction was recovered by centrifugation at 700 rpm for 4.0 min. This process was repeated four times, in order to guarantee obtaining samples in a pure form, free from quartz, carbonates, calcites, iron hydroxide, and organic metals. The suspension was collected, following evaporation of water at 35°C on a hot plate. The samples were dried in an oven at 60°C, ground and sieved using a 63 $\mu$m mesh, and stored in tightly closed plastic bottles for use in the experiments.

*2.2. Sodium Activation of the Purified Bentonite.* The purified bentonite (PB) was prepared for sodium activation: 17 g ± 0.01 g of the purified sample was weighed into a flask and 250 mL of 1.0 m NaCl (Puriss) was added. The resulting suspension was stirred at room temperature for 48 h. When the mixing process was completed, the resulting slurry was filtered by a Büchner funnel; then, it was washed with deionized water several times until it was released from $Cl^{-1}$ ions against a 5% $AgNO_3$ (Puriss) solution. After drying the sample at 70°C for 24 h, it was regrinded to reach 300 $\mu$m particle size and stored in tightly closed plastic bottles to be used in adsorption studies.

The following reaction had occurred:

$$\text{Ca} - \text{Bent} + 2\text{Na}^{+} \longrightarrow 2\text{Na} - \text{Bent}\,(\text{AJB}) + \text{Ca}^{2+}. \quad (1)$$

FTIR spectroscopy (Thermo Nicolet NEXUS 670 Spectrophotometer), XRD (Philips X pert pro), TGA (NETZCH STA 409 PG/PC Thermal Analyzer), and BET surface area analysis (Gemini VII from micromeritics) were handled for characterization of both PB and AJB.

*2.3. Handling of Olive Mill Wastewater Samples.* OMW was obtained from three different olive oil mills located at Jerash city,;the preservation, pretreatment, and physicochemical characterization of the OMW samples were operated as executed in the previous work [2]. Fresh OMW was fully characterized before and after treatment. Total dissolved solid (TDS) was measured using a Crison PL-700AL meter. Alkalinity, total of chlorine, phosphate, nitrate, and chemical oxygen demand (COD) concentrations were determined using A COD and multiparameter bench meter, PN HI83099-02. Sodium ($Na^+$) and potassium ($K^+$) ions concentrations were determined using a flame photometer (Corning 400). TPC were evaluated by UV-VIS spectrophotometer (Varian Cary 100) using the Folin–Ciocalteu method. Briefly, 2.5 mL of 0.2 N of Folin–Ciocalteu reagent was mixed with 0.5 mL of the OMW sample. The mixture was kept in the dark for 5 min. Then, 2 mL of a sodium carbonate solution (75 g/L) was added; the reaction was left in the dark at 25°C for 1 h and then centrifuged at 8000 rpm for 5 min. The absorbance of the supernatant was read at $\lambda = 765$ nm. Gallic acid was used as a standard for the calibration of the method. TPC were expressed as gallic acid equivalents in gram per liter (g GAE/L residue) [37].

*2.4. Adsorption Experiments.* Batch adsorption experiments were performed. The effect of AJB dosage, the initial concentration of TPC, and the solution temperature, on the percentage removal, were studied.

The concentration of adsorbate retained in the adsorbent phase ($q$, mg $g^{-1}$) was calculated from the following equation [38]:

$$q = \frac{(C_i - C_e)}{m} * V, \tag{2}$$

where $q$ is the adsorbent phase concentration after equilibrium (mg adsorbate/g adsorbent), $C_i$ and $C_e$ are the initial and final (equilibrium) concentrations, respectively, of adsorbate in solution (mg/L), $V$ is the solution volume (L), and $m$ is the adsorbent mass (g). Percentage (%) removal of adsorbate was calculated using the following equation [39]:

$$\%\text{removal} = \frac{(C_i - C_e)}{C_i} * 100. \tag{3}$$

## 3. Results and Discussion

*3.1. Characterization of PB and AJB Adsorbents*

*3.1.1. FTIR Spectra.* The FTIR analysis of the PB and AJB was utilized to determine the functional groups on the surface of bentonite responsible for adsorption and to explore the effect of sodium activation on its chemical composition, which is shown in Figure 2.

From the PB spectrum, absorption bands resulting from bending vibrations of Si-O groups are found in the 550–400 $cm^{-1}$ region. The bands due to Si-O-Al and Si-O-Si deformations in the spectra occur near 530 and 460 $cm^{-1}$, respectively [40]. The spectrum also contains a band at 706, 800, and 2355 $cm^{-1}$ which is all attributed to quartz [41, 42]. A broad complex band near 1030 $cm^{-1}$ is related to stretching vibrations of Si O groups [43]. On the other hand, the peak at 1641 $cm^{-1}$ is for H-O-H bending, and the stretching vibration of OH appears at around 3451 $cm^{-1}$. The adsorption band at 3616 $cm^{-1}$ in the spectrum is assigned to stretching vibrations of the structural OH groups of dioctahedral bentonite.

After sodium activation, the most significant change was a decrease in the intensity of the band of the Si-O stretching region at 1030 $cm^{-1}$. This means that upon the activation process, there is a possibility of the formation of three-dimensional networks of amorphous silica, which may expose more adsorption sites, which may cause damage to the tetrahedral layer. The intensity of bending and stretching bands characterized the octahedral sheet for Al-Al-OH at a 1641 $cm^{-1}$ decrease, which indicates the destruction of the octahedral layer. Additionally, a sharp decrease in the absorption band attributed to the OH vibration at 3616 $cm^{-1}$ is due to the removal of the octahedral cations, thus causing the loss of water and hydroxyl groups coordinated to them [44]. The decrease in the characteristic band at 3451 $cm^{-1}$ represents the fundamental stretching vibrations of different -OH groups present in Fe-OH-Al, Al-OH-Al, and Mg-OH-Al in the octahedral layer [45] which confirms the disfiguration of the layer. Furthermore, regarding quartz bands, the disappearance of the band at 2355 $cm^{-1}$ is noted as well as a decrease in the intensities of bands at 706, 800 $cm^{-1}$, which offers a strong indication that the activation process improves the purity of the bentonite.

During the activation process, most band positions did not change, thus indicating that the basic bentonite structure did not interrupt.

*3.1.2. X-Ray Diffractograms.* The X-ray diffraction patterns of PB and AJB samples are illustrated in Figure 3. Patterns of PB montmorillonite were the main mineral. However, minor amounts of quartz, kaolinite, gypsum, and cristobalite were also identified [46].

As seen from the AJB patterns, the XRD results indicate that changes in the structure of PB are induced by adding NaCl. Quartz is not present in the AJB sample; the peaks of quartz are diminished. The main montmorillonite peaks are present. Two distinct diffraction lines belonging to crystalline NaCl (35 and 55 Å) are seen, thus proving the accumulation of crystalline NaCl [47]. X-ray results of activated bentonite show there is a shift in the position of a few peaks (for example, 31.2–26.6 Å). After the addition of NaCl, the $Na^+$ ions are absorbed to the surface of the montmorillonite crystal grains to form a hydrated shell [48]. This is an indication of the dissolution of the tetrahedral and octahedral sheets and subsequent release of the structural cations, that is, these cations have been eliminated from the octahedral positions, thereby exchanging with $Na^+$ ions. Moreover, the interlamellar spacing between crystal grains is compressed [49]. The chemical composition and inner structure of AJB are changed. Distinctly, XRD analysis provides good evidence that the adsorptive power of AJB has increased.

Clearly, the activation process causes a decrease in peak intensity. This mostly occurs in the case of montmorillonite, which means a reduction in its content and also the disappearing of the quartz impurity content. Furthermore, the peaks of PB patterns have relative symmetry, but the peaks of AJB patterns are moving to more dissymmetry. Also, the appearance of splitting in some peaks, which is an indication of phase transformation to a lower symmetry or partial distortion of its structure, indicates that small distortions can often be observed with peak broadening. These characteristics apparently indicate that bentonite is well activated by $Na^+$ ions.

The reduction in intensity and increase in the width of peaks at 24.1 Å indicates that the crystallinity of the bentonite is considerably affected by activation, and thus, the bentonite crystalline structure is decomposing, which means that the activation process is accompanied by the appearance of an amorphous phase, as confirmed by IR results.

*3.1.3. Thermogravimetric Analysis (TGA).* Thermogravimetric analysis was undertaken to investigate the effect of activation of bentonite with NaCl. Figure 4 shows a distinct endotherm with a maximum between 30°C and 200°C that corresponds to the release of physically adsorbed water and the dehydration process. Dehydroxylation was executed with more and more favorable temperatures, ranging from 325 to 720°C. The decomposition of chemically bound water (OH-) is detected by an endothermic change with a maximum at 350°C. The dissociation of accumulated NaCl crystals is confirmed at 800°C [50]. The total mass losses within the temperature interval of 30–200°C of PB is much more than ABJ. Beyond this temperature, there are higher mass losses for AJB, and this is attributed to the dissociation of crystalline NaCl at 800°C. This finding confirms those of the XRD results that show a partial deterioration of the AJB microstructure. The results obtained confirm the formation of NaCl crystals in the AJB, where the accumulated NaCl crystals have a destructive effect mainly on the bentonite microstructure and a secondary effect on its increase in permeability. This is enhancing its adsorption capacity toward phenolic compounds, heavy metal ions, and other pollutants. Furthermore, the TGA result is in clear agreement with the FTIR and XRD studies, which indicate consecutive changes of the bentonite sheet upon the activation process.

*3.1.4. BET Surface Area.* The results of the BET analysis show that the surface area increases with increasing Na on the surface of bentonite. The surface area increases from 66.2 $m^2\ g^{-1}$ for PB to 249.6 $m^2\ g^{-1}$ for AJB. The improved surface area indicates the number of active sites increases on the surface of the adsorbent, which improves the enhancement in adsorption efficiency [51].

In studying the adsorption and swelling properties of the clay-water system, one type of swelling, commonly known as the interlayer or interlamellar swelling, involves the expansion of the crystal lattice itself, as found in montmorillonite [52]. It is known that the swelling properties of bentonite depend on the type of exchangeable cations, whether $Na^+$ or $Ca^{2+}$. Calcium ions have a higher charge and smaller diameter than sodium ions, and as a result, they tend to interact more strongly with the aluminosilicate platelets, thus making them less disposed to swelling. Sodium ions hydrate more readily causes the bentonite to swell more, so any effort to increase the concentration of $Na^+$ ions will improve the swelling properties of bentonite [53]. This is perfectly consistent with the obtained XRD result. However, improved swelling of bentonite after activation is expected to yield an increase in pore size and thus an increase in adsorption capacity. As a result, it improves the removal of phenolic compounds and other pollutants.

*3.2. Characterization of OMW.* The characteristics of the studied crude and treated OMW are summarized in Table 1. The analysis of the OMW shows that it is composed mainly of organic compounds and inorganic compounds (mineral salts). Among the different mineral salts present in OMW, potassium has the highest concentration. Other cations and anions are also found in OMW at lower concentrations. Also, the high phenol content of OMW contributes to the high soluble COD of OMW. Total dissolved solids content is also high, as well as the phosphate content being significant. All the above parameters must be taken into consideration in the design of a well-integrated treatment process for OMW.

It is worth noting here that the parameter values are in good agreement with those reported in the literature. Clearly, using PB for OMW treatment is essential due to significant differences between its properties. Furthermore, it is noticed that the percentage removal increases vigorously and continuously throughout the use of AJB adsorbent, and this is a good indication that simple activation of bentonite can result in a good result on its adsorption behavior. Therefore, AJB adsorbent provides a valuable solution for the treatment and recyclability of OMW.

*3.3. Adsorption Experiments*

*3.3.1. TPC Removal.* Both PB and AJB were tested for the removal of TPC, and batch experiments were performed, where several parameters were tested, to determine the adsorption effectiveness. Different adsorbent dosages (0.1, 0.5, and 1.0 g) were mixed with 10 mL of OMW with different initial TPC concentrations (1215.16, 1340.64, 1442.00, and 1563.43 mg/L) at different temperatures (293, 303, 313, and 323 K). OMW and adsorbent were stirred in Erlenmeyer flasks continuously for 3 h. After shaking, samples were filtered using a 0.45 $\mu$m microfilter and then analyzed by a UV-VIS spectrophotometer at $\lambda = 765$ nm to measure the concentration of TPC. Finally, all analytical methods were applied at least in triplicate.

The adsorption amount of TPC using AJB is larger than the unactivated one, as shown in Figure 5. The proposed explanation of the enhanced adsorption involves bentonite having a large specific surface area and pore spaces, and it is based on the diffuse double layer theory, which predicted that double layer thickness decreases with increasing pore-

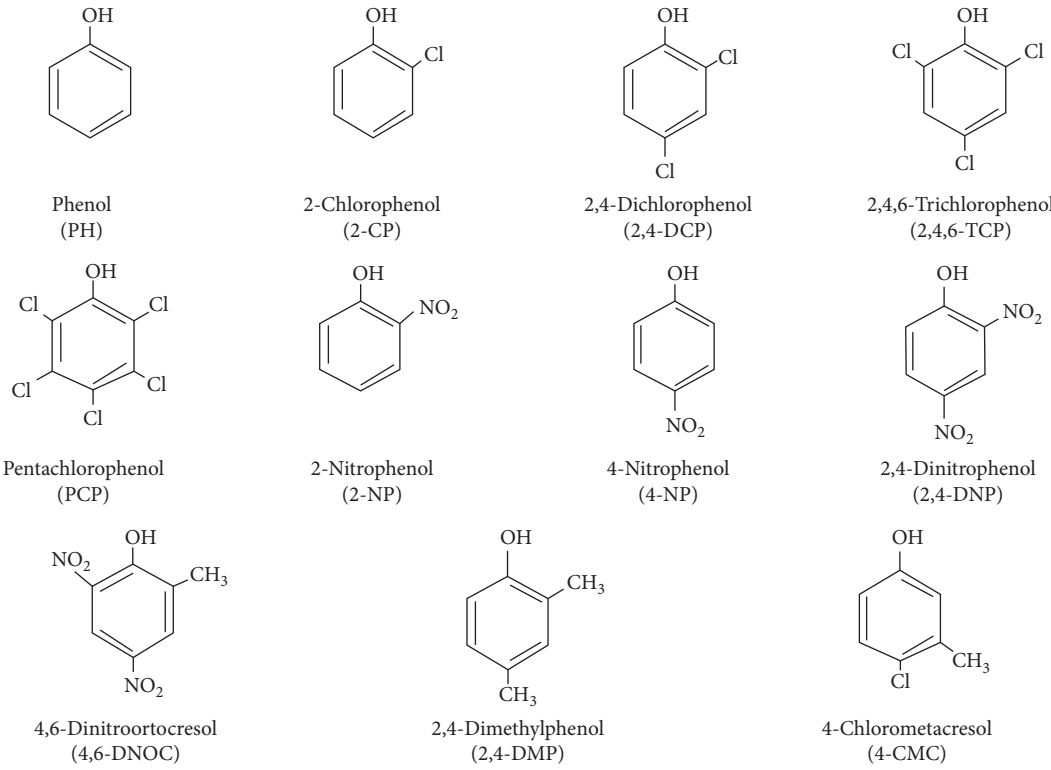


Figure 1: Phenolic compounds structures considered priority contaminants by US EPA [29].

solution concentration [66]. Moreover, sodium chloride dissociates into $Na^+$ and $Cl^-$ in an aqueous solution. There is a strong electrostatic field around the anions and cations, and thus, an oriented array of water molecules is formed around these ions. The existence of ions enhances the combining powers between water molecules and phenolic compounds. On the other side, the hydraulic conductivity of the bentonite increases as the void ratio increases. Also, at a given void ratio, the hydraulic conductivity of the bentonite increases, as the ionic strength increases. This trend for increasing hydraulic conductivity may result from the influence of the permanent on effective porosity (the pore space available for conductive flow), which concludes that increasing the concentration of salts, such as NaCl, leads to an increase in permeability in bentonite due to a decrease in interparticle repulsion among negatively charged plates [67]. As a result of the activation of bentonite by NaCl, adsorption capacity increases towards TPC.

Similar behavior was reported for TPC adsorption by hydrochloric acid-activated bentonite. Other than that, AJB by sodium ions provides a higher adsorption capacity [2]. It is thought that the presence of NaCl crystals has an effect on its increase in permeability, which leads to an increase in the cation exchange capacity [68]. Furthermore, the possible mechanism of the adsorption process of TPC onto AJB likely to be ionic interactions between phenolate ions and sodium on the surfaces of the prepared adsorbent Na-Bent (AJB) and sodium phenoxide ($C_6H_5ONa$) will be formed [69]. Sodium atoms presented on AJB play an essential role in enhancing the absorption capacity via the electrostatic attraction [70].

*(1) Effect of Adsorbent Dosage on Adsorption of TPC*. The experimental data regarding the effect of adsorbent dosage on the percentage removal of TPC by AJB is shown in Figure 6. A series of batch experiments were carried out by contacting different amounts of AJB with 10 mL of OMW, with a constant initial TPC concentration of 1340.64 mg/L. The contact time was made for 3 h and at different four temperatures 293, 303, 313, and 323 K.

The results show that increasing the dosage of AJB increased in the percentage removal of TPC. However, the adsorption capacity of AJB increases, and this could be due to an increase in the surface area and the availability of more active sites on the surface of AJB [71]. Moreover, the adsorption capacity for AJB is greater than PB at constant temperature and dosage, which indicates that the bentonite is well activated by NaCl. Therefore, to reduce the bentonite dosage, it is necessary to modify it into superior Na-bentonite.

By comparison of these obtained results, with those in the previously reported work, the percentage removal of TPC at the same adsorbent dosage and all temperatures is higher while using AJB activated by sodium ions rather than by acid activation of bentonite [2].

*(2) Effect of Initial TPC Concentration*. The initial TPC concentration is a very important factor to be explored in adsorption studies, as most contaminated OMW usually presents different concentrations of TPC. The effect of initial TPC concentration on the adsorption capacity and percentage removal is shown in Figure 7. The operating

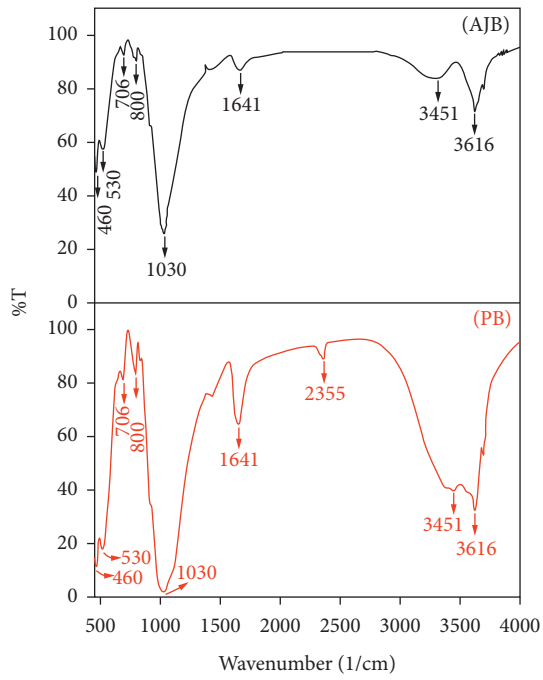


Figure 2: FTIR spectra of PB and AJB.

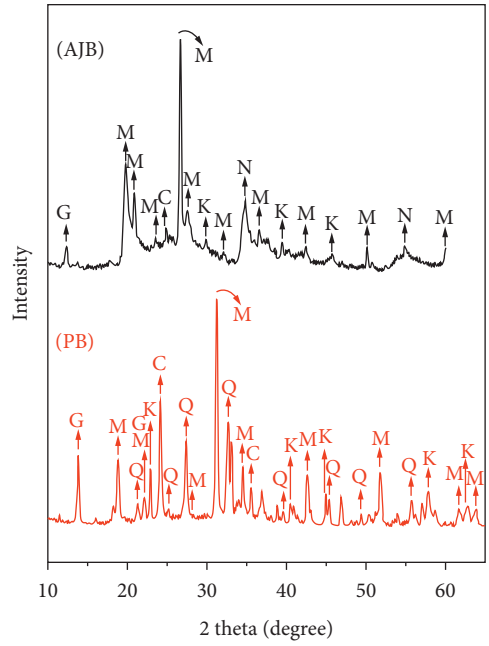


N: sodium chloride
M: montmorillonite
C: cristobalite
K: kaolinite
G: gypsum
Q: quartz

Figure 3: X-ray diffraction patterns of the PB and AJB.

conditions for the batch experiments were 1.0 g of AJB per 10 mL of OMW, and the contact time was 3 h at 303 K.

First, an increase in adsorption capacity with an increase in initial TPC concentration was observed. This may be explained by the presence of more TPC in the solution available for binding onto the active sites of the AJB. Consequently, the adsorption reached a saturation value. Indeed, the initial TPC concentration provides an important driving force to overcome all mass transfer resistance. Hence, a higher initial concentration of TPC tends to enhance the adsorption capacity. A similar phenomenon was observed for the adsorption of phenol onto organobentonite

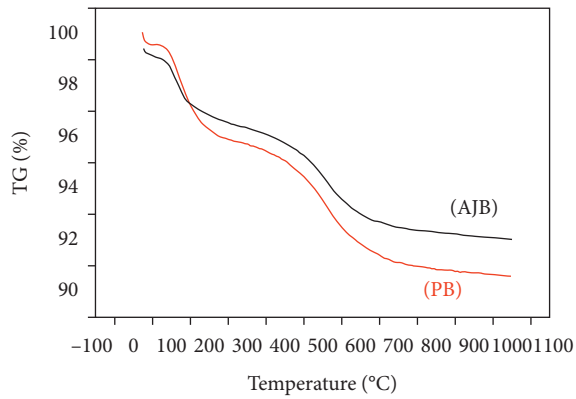


Figure 4: TGA curves of PB and AJB.

Table 1: Main characteristics of the OMW sample untreated and treated with PB and AJB.

| Parameters | Untreated OMW | Literature ranges values | Reference | Treated OMW with PB | Treated OMW with AJB | % removal using PB | % removal using AJB |
|---|---|---|---|---|---|---|---|
| Sodium ($Na^+$), mg $L^{-1}$ | 297.9 | 200–570 | [54, 55] | 186.4 | 119.4 | 37.4 | 59.9 |
| Potassium ($K^+$), mg $L^{-1}$ | 6366.3 | 639–10800 | [56, 57] | 4075.1 | 2606.3 | 35.9 | 59.1 |
| TPC, g GAE/L | 1.34 | 0.26–10.7 | [56, 58] | 0.85 | 0.44 | 36.6 | 67.2 |
| Alkalinity ($CaCO_3$), mg $L^{-1}$ | 2000 | 3150–9070 | [59] | 1500 | 500 | 25.0 | 75.0 |
| Total chlorine, mg $L^{-1}$ | 20 | 33.3–142.7 | [60] | 15 | 7 | 25.0 | 65.0 |
| Phosphate ($PO_4^{3-}$), mg $L^{-1}$ | 4120 | 31.8–1820 | [61] | 460 | 230 | 88.8 | 94.4 |
| Nitrate ($NO_3^-$-N), mg $L^{-1}$ | 360 | 350–390 | [62] | 230 | 120 | 36.1 | 66.7 |
| COD, mg $L^{-1}$ | 12000 | 1900–220000 | [63, 64] | 7030 | 1182 | 41.4 | 90.2 |
| TDS, mg $L^{-1}$ | 34700 | 5900–103200 | [65] | 13140 | 11899 | 62.1 | 65.7 |

[72]. Meanwhile, the percentage of removal decreased gradually with an increase in the initial TPC concentration. This decrease occurs because all adsorbents have a limited number of active sites, and at higher concentrations, the active sites become saturated [73]. Besides, the % removal of TPC was calculated concerning the initial concentration ($C_i$) of adsorbate in solution as clarified in the equation (3); therefore, as ($C_i$) increased in the denominator, the % removal will be decreased.

The following flow chart shows steps and quality controls for producing reliable and comparable information of assaying the concentration of TPC using AJB adsorbent for wastewater treatment as shown in Figure 8.

*3.3.2. Adsorption Isotherms.* The adsorption isotherms for TPC removal by AJB were investigated using different initial concentrations at the adsorbent mass of 1.0 g at 293, 303, 313, and 323 K and for a period of 3 h. Later, the data obtained were fitted to the Langmuir and Freundlich isotherms.

The Langmuir isotherm assumed that the monolayer adsorption of adsorbate onto a homogeneous adsorbent surface takes place with a single coating layer on this surface [74]. Moreover, there is no lateral interaction between the adsorbed molecules. The linear form of the Langmuir isotherm model can be expressed as [75, 76]

$$\frac{C_e}{q_e} = \frac{1}{K_L q_m} + \frac{C_e}{q_m}, \tag{4}$$

where $q_e$ is the equilibrium adsorption capacity (mg/g), $C_e$ is the equilibrium concentration of TPC (mg/L), $q_m$ is a maximum adsorption capacity (mg/g), and $K_L$ is the adsorption equilibrium constant (L/mg).

The linear form of the Langmuir isotherm is shown in Figure 9. The correlation coefficients, $R^2$ >0.99 at all temperatures, indicate that the adsorption was a good fit for this model.

The maximum adsorption $q_m$ for TPC onto AJB equals to 8.81 mg/g. The adsorption process can be evaluated to see whether it is favorable by the use of a Langmuir dimensionless separation factor $R_L$ defined as [77]

$$R_L = \frac{1}{1 + K_L C_o}, \tag{5}$$

where $C_o$ (mg/L) is the initial TPC concentration in solution. If the value of $R_L$ is less than 1.0, the adsorption is considered

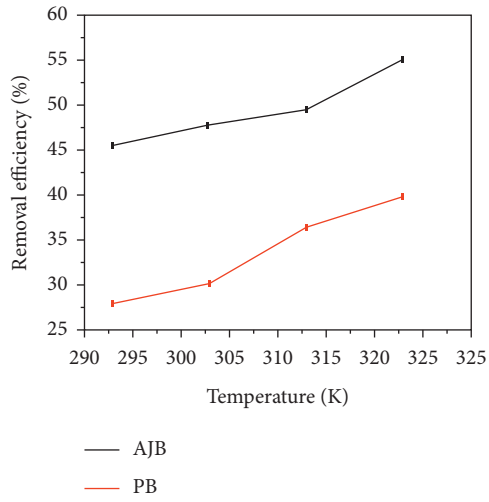


Figure 5: Comparison of the percentage removal of TPC by PB and AJB. Mass of adsorbent = 1.0 g, initial TPC concentration, 1340.64 mg/L, 10 mL of OMW, and contact time = 3 h.

to be favorable, but it is unfavorable if $R_L$ is greater than 1.0. The calculated $R_L$ values at different concentrations fall within the range of 0.098–0.122 (Table 2), thus indicating a favorable adsorption process.

The Freundlich isotherm is based on multilayer adsorption on heterogeneous surfaces [78]. The linear form of Freundlich can be represented as

$$\log q_e = \log K_F + \frac{1}{n}\log C_e, \quad (6)$$

where $K_F$ and $n$ are the Freundlich adsorption constants showing the adsorption capacity (mg/g) and intensity, respectively, which can be determined by the linear plot of log $q_e$ versus log $C_e$.

The adsorption Freundlich isotherm obtained for TPC onto AJB is shown in Figure 10, and the isotherm parameters for both models are presented in Table 3.

The obtained values of $n$ exhibited intense change at higher temperatures. All $n$ values were greater than one, indicating favorable adsorption of TPC [79]. Also, the high correlation coefficient values ($R^2$) of the Langmuir and Freundlich models indicate that the experimental data are well fitted by both models.

Comparison of AJB with other adsorbents is necessary. Table 4 provides the adsorption capacities for TPC on different types of adsorbents as reported in the literature. It is thought that those adsorbent's properties have a significant effect on its efficiency, and experiment conditions may cause different results. Based on that, it seems that the AJB for TPC removal is a promising effective adsorbent. Results in Table 4 show that AJB has a high adsorption capacity compared to a wide range of adsorbents. On the other hand, the adsorption capacity of macroporous resins XAD-16 is higher than that of prepared AJB.

The activation by sodium ions has the potential to produce a high surface BET area for AJB (the surface area increases from 66.2 to 249.6 $m^2\ g^{-1}$) characterized by high uptake capacity for organic compounds compared to other adsorbents. However, very few studies reportedly tested the adsorption of TPC onto the bentonite produced via this activation method. Among this method, the sodium ions activation method will gain more attention from researchers. This has been attributed to fact that such method is fast, ease of operational conditions, and characterized by cost savings over the conventional techniques [87].

### 3.3.3. Thermodynamic Studies

*(1) Effect of Temperature on Adsorption of TPC.* In order to determine the effect of temperature on the adsorption of TPC onto AJB, experiments were run with four different values: 293, 303, 313, and 323 K. From the curves of Figure 11, we can notice that the percentage of efficient removal of TPC increases with temperature, which indicates that the adsorption process is endothermic. This could be due to increasing the mobility of the TPC, thus gaining more kinetic energy to diffuse from the bulk phase to the solid phase, with an increase in solution temperature. Furthermore, there is an increase in the number of surface active sites for the adsorption with increasing temperature, as a result of the dissociation of some of the surface components onto AJB [88, 89]. On the other hand, $K_L$ values are directly proportional to the temperature, as shown in Figure 11. $K_L$ is the Langmuir equilibrium constant related to the affinity of binding sites and energy of sorption, equation (4). Again, TPC has a good affinity to the AJB surface and increases gradually with increasing temperature. Similarly, at constant initial TPC concentration (1340.64 mg/L) and fixed dosage of both adsorbents (1 g), as clearly observed in Figure 11, the percentage removal of TPC using PB adsorbent increases with increasing temperature.

The temperature has an obvious effect on sodium modification of the bentonite, and $Na^+$ in the diffusion layer present has a trend of moving to bentonite surfaces. The migration of $Na^+$ is increased, which increases the content of

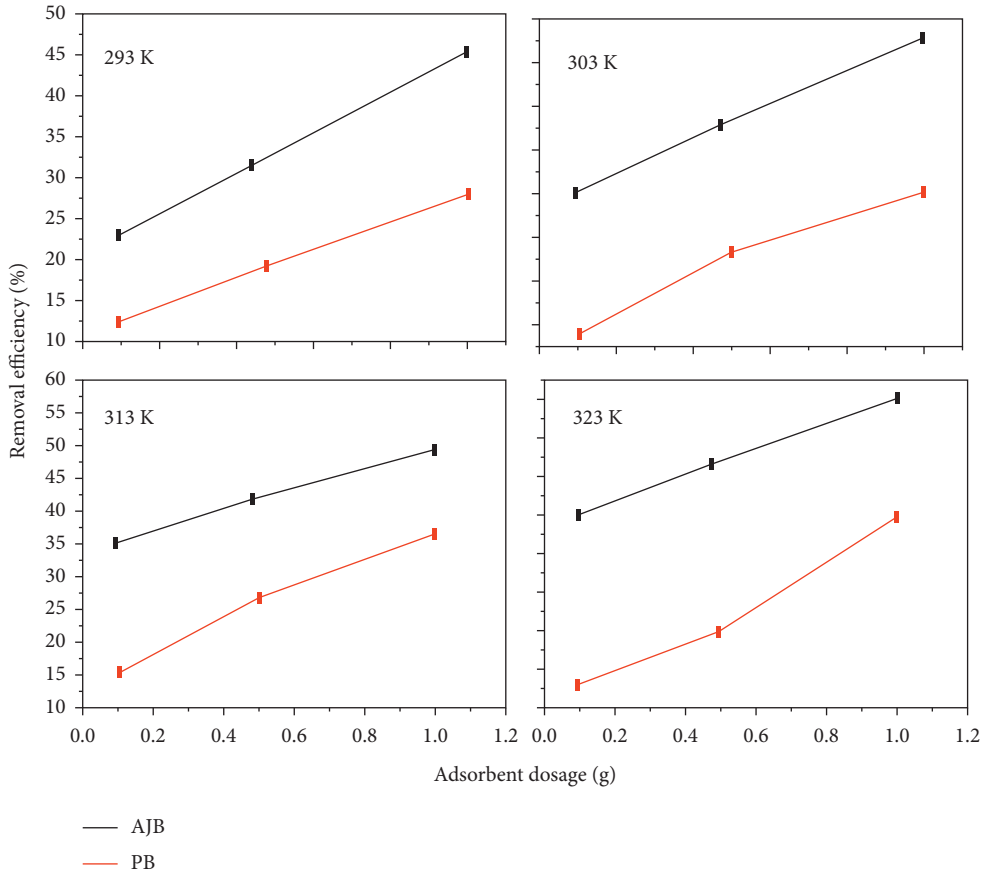


Figure 6: Effect of adsorbent dosage on the percentage removal of TPC at different temperatures.

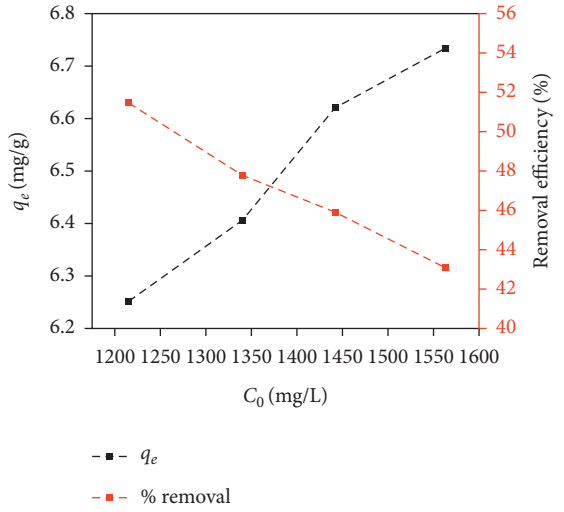


Figure 7: Effect of initial TPC concentration on the adsorption capacity and the percentage removal of TPC.

Na + on the bentonite surface. Therefore, the reaction velocity between $Na^+$ and $Ca^{2+}$ is growing [90].

Comparing the results of percentage removal of TPC obtained by using AJB, with those in the previously reported study, AJB presents a good adsorption capacity rather than the acid-activated Jordanian bentonite [2]. Hence, AJB utilization for the removal of TPC is very promising.

To evaluate the feasibility of the adsorption process, thermodynamic parameters, where $\Delta G^\circ$ is the Gibbs free energy (kJ/mol), $\Delta H^\circ$ is the standard enthalpy (J/mol), and

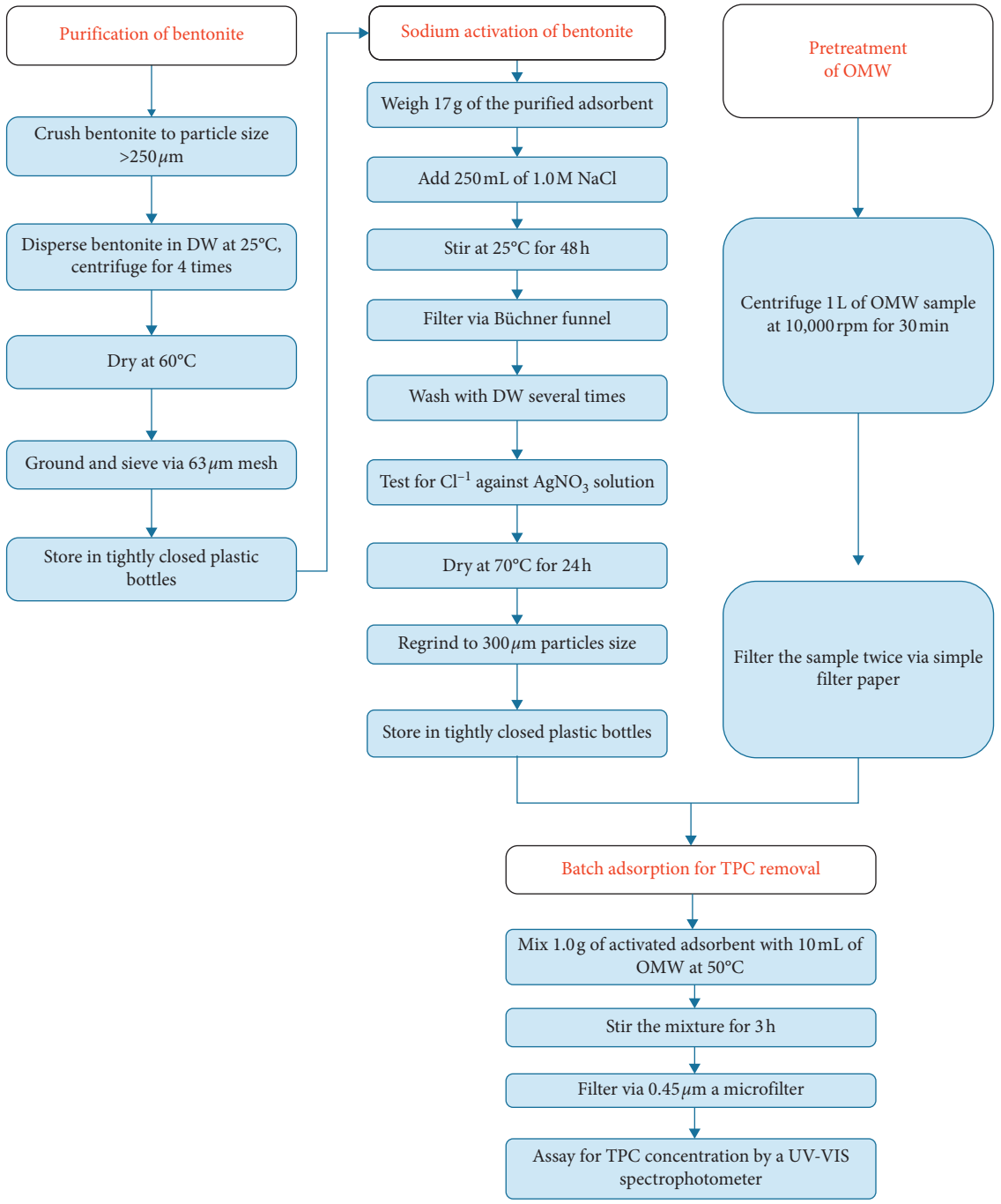


Figure 8: Protocol for OMW treatment and assaying for TPC concentration using AJB adsorbent.

$\Delta S^{\circ}$ is the standard entropy (J/mol K), were calculated from the curve relating the distribution coefficient (K) as a function of temperature, using the following equations [91]:

$$\Delta G^{\circ} = -\mathrm{RT} \ln K,$$
$$\ln K = \frac{\Delta S^{\circ}}{R} - \frac{\Delta H^{\circ}}{\mathrm{RT}}, \quad (7)$$

where $R$ is the gas constant (8.3145 J.mol$^{-1}$.K$^{-1}$), and $T$ is the temperature in Kelvin. The values of $\Delta H^{\circ}$ and $\Delta S^{\circ}$ were determined from the slope and intercept values of the straight line of plotting ln $K$ versus $1/T$, respectively. According to the data presented in Table 5, the spontaneity of the adsorption process is established by a decrease in $\Delta G^{\circ}$ values, in addition to spontaneity increases as the temperature of the solution increases, which means that, as the adsorption process becomes more favorable, the negative values of $\Delta G^{\circ}$ indicate that the adsorption of the TPC is spontaneous and favorable [92]. The positive value of $\Delta H^{\circ}$ shows that the adsorption process is endothermic in nature [93]. This is following increasing adsorption equilibrium with increasing temperature. The positive value of $\Delta S^{\circ}$

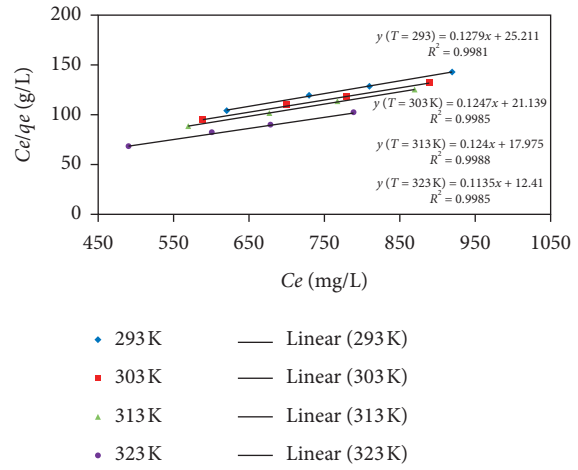


Figure 9: Langmuir plot for the adsorption of TPC onto AJB. Adsorbent dosage = 1.0 g 10 mL of OMW, pH = 6, contact time = 3 h.

Table 2: Calculated values of separation factor $R_L$ for the adsorption of TPC onto AJB at 303 K.

| $C_o$ | 1215.16 | 1340.64 | 1442.00 | 1563.43 |
|---|---|---|---|---|
| $R_L$ | 0.1224 | 0.1123 | 0.1052 | 0.0978 |

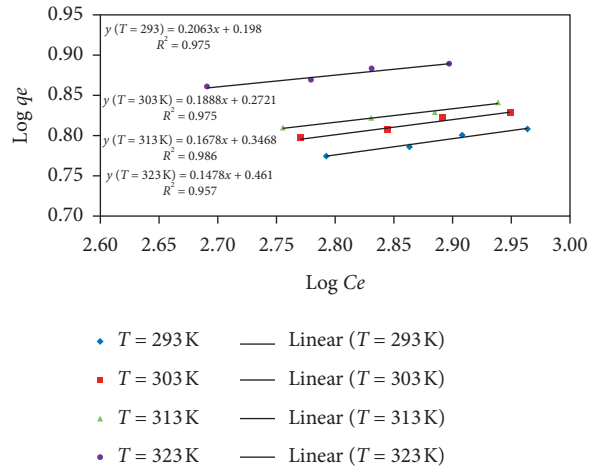


Figure 10: Freundlich plot for the adsorption of TPC onto AJB. Adsorbent dosage = 1.0 g 10 mL of OMW, pH = 6, contact time = 3 h.

Table 3: Langmuir and Freundlich isotherm parameters for the adsorption of TPC onto AJB.

| $T$ (K) | Langmuir isotherm | | | Freundlich isotherm | | |
|---|---|---|---|---|---|---|
| | $q_m$ | $K_L$ | $R^2$ | $n$ | $K_F$ | $R^2$ |
| 293 | 7.8168 | 0.0051 | 0.9981 | 4.8481 | 1.5774 | 0.9754 |
| 303 | 8.0201 | 0.0059 | 0.9985 | 5.2958 | 1.8710 | 0.9753 |
| 313 | 8.0640 | 0.0069 | 0.9988 | 5.9604 | 2.2222 | 0.9860 |
| 323 | 8.8128 | 0.0091 | 0.9985 | 6.7648 | 2.8905 | 0.9576 |

reflects an increase in the randomness at the interface between AJB and the phenolic solution during the adsorption process. This suggests that some structural changes occur on the adsorbent, in addition to the adsorbate, due to the exchange of the phenolic compounds with more mobile ions present on the AJB, which would cause an increase in the entropy during the adsorption process [94].

Moreover, the $\Delta H^{\circ}$ value was 559.47 kJ/mol, thus indicating that the adsorption of TPC onto AJB involved chemical adsorption. Value of enthalpy within the range

Table 4: Comparison of adsorption capacities of different adsorbents for TPC reported in the literature.

| Adsorbent | Adsorption capacity $q_m$ (mg/g) | Reference |
|---|---|---|
| Polydimethylsiloxane/oxMWCNTs | 4.39 | [80] |
| Olive pomace | 11.40 | [81] |
| HyAlFe-Mt | 10.2 | |
| HyAlFe | 15.7 | [82] |
| Silver and titanium oxides-doped activated carbon | 11.0168 | [83] |
| Macroporous resins XAD16 | 16 | [84] |
| Nonionic styrene-divinylbenzene resin (XAD1) | 3.4 | |
| Nonionic styrene-divinylbenzene resin (XAD2) | 7.6 | |
| Strong basic anion exchange resin (IRA1) | 2.1 | [85] |
| Strong basic anion exchange resin (IRA2) | 0.9 | |
| XAD16HP | 2.30 | |
| SP700 | 2.59 | [86] |
| AJB | 8.81 | Present study |

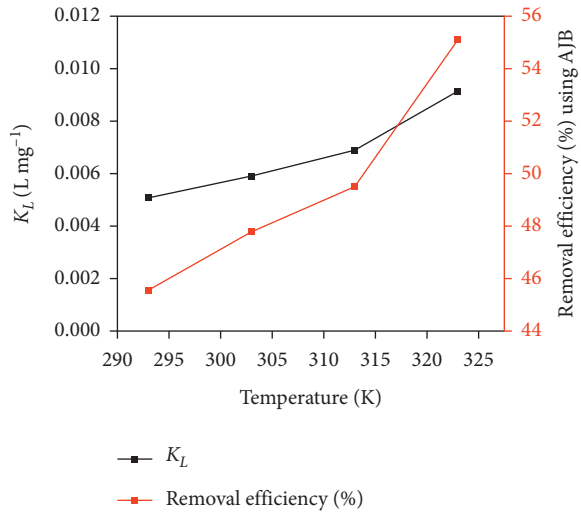


Figure 11: Effect of solution temperature on the percentage removal of TPC and the Langmuir equilibrium constant $K_L$ using AJB.

Table 5: Thermodynamic parameters of adsorption of TPC onto AJB.

| $T$ (K) | $\Delta G^\circ$ |
|---|---|
| 293 | 26.22 |
| 303 | 13.90 |
| 313 | −5.22 |
| 323 | −28.21 |
| $\Delta H^\circ = 559.47$ | $\Delta S^\circ = 1.81$ |

2.1–20.9 kJ/mol indicates physical sorption, and value over 20.9 kJ/mol indicates chemisorption [95]. Therefore, the process is irreversible [96]. Thus, the adsorption mechanism involves valences forces and chemical bond [75, 97].

According to the results obtained from this work, by using effectively-prepared AJB adsorbent, it is favorable in terms of both economic and environmental features, and it could improve adsorption for the removal of hazardous materials, such as phenolic compounds from industrial effluents such as OMW. Furthermore, this study is expected to be of great benefit because all these processes are interrelated; especially given that there are no previous studies on Jordanian bentonite that considered all these processes.

## 4. Conclusion

The management of produced OMW is a particularly unsolved problem, especially in Jordan, due to its high content of phenolic compounds, their physicochemical composition, and the implicit toxic merits. More effective, simple, available, low cost, and environmentally friendly methods are needed mainly in developing countries. The current study presents a successful method for the activation of Jordanian bentonite using sodium chloride. The AJB has been examined as an adsorbent for OMW treatment. The physicochemical analysis appears to show a good performance for AJB, which can help reduce environmental

damage, prevent groundwater contamination, and provide an alternative approach for olive mills, in regards to safe utilization of OMW. Moreover, AJB shows great potential for the removal of phenolic compounds pollutants. Results show the percentage of removal for phenolic compounds can be considered as satisfactory. Improvement of the adsorption efficiency is achieved by optimized different parameters, which were as follows: the adsorbent dosage was 1.0 g, initial TPC concentration was 1215.16 mg/L, and the temperature of the solution was 323 K. On the other hand, its equilibrium adsorption was well fitted to the Langmuir and Freundlich models. Thermodynamics studies have confirmed that the adsorption process was spontaneous and endothermic in nature.

Notably, the AJB shows a substantially higher adsorption capacity compared to PB. This study provides a feasible method for utilizing activated bentonite for application in wastewater treatment.

## Data Availability

All data generated or analyzed during this study are included within the article.

## Conflicts of Interest

The authors declare that there are no conflicts of interest.

## Acknowledgments

The authors are grateful for Support to Research and Technological Development and Innovation Initiatives and Strategies in Jordan (SRTD II) and the European Union Funded Project, Budget line BGUE-2011-19.080101-CI-DEVCO, Reference: SRTD/2014/GRT/AR/2321, for having funded the project, in addition to Jerash University, and Mr. Mouhamad Shehabat for language editing.

## References

[1] K. Al-Essa, "Olive mill wastewater treatment using a simple raw and purified Jordanian bentonite based low-cost method," *Asian Journal of Chemistry*, vol. 30, no. 2, pp. 391–397, 2018.

[2] K. Al-Essa, "Activation of Jordanian bentonite by hydrochloric acid and its potential for olive mill wastewater enhanced treatment," *Journal of Chemistry*, vol. 2018, Article ID 8385692, 10 pages, 2018.

[3] W. Bekele, G. Faye, and N. Fernandez, "Removal of nitrate ion from aqueous solution by modified ethiopian bentonite clay," *International Journal of Research in Pharmacy and Chemistry*, vol. 4, no. 1, pp. 192–201, 2014.

[4] R. Resende, P. Leal, D. Pereira, R. Papini, and Z. Magriotis, "Removal of fatty acid by natural and modified bentonites: elucidation of adsorption mechanism," *Colloids and Surfaces A: Physicochemical and Engineering Aspects*, vol. 605, pp. 1–8, 2020.

[5] J. Yang, K. Shi, X. Gao, X. Hou, W. Wu, and W. Shi, "Hexadecylpyridinium (HDPy) modified bentonite for efficient and selective removal of 99Tc from wastewater," *Chemical Engineering Journal*, vol. 382, pp. 1–34, 2020.

[6] M. Khatamian, B. Divband, and R. Shahi, "Ultrasound assisted co-precipitation synthesis of Fe3O4/bentonite nanocomposite: performance for nitrate, BOD and COD water treatment," *Journal of Water Process Engineering*, vol. 31, pp. 1–12, 2019.

[7] P. Choudhury, P. Mondal, and S. Majumdar, "Synthesis of bentonite clay based hydroxyapatite nanocomposites cross-linked by glutaraldehyde and optimization by response surface methodology for lead removal from aqueous solution," *RSC Advances*, vol. 5, pp. 100838–100848, 2015.

[8] B. Meng, Q. Guo, X. Men, S. Ren, W. Jin, and B. Shen, "Modified bentonite by polyhedral oligomericsilsesquioxane and quaternary ammonium salt and adsorption characteristics for dye," *Journal of Saudi Chemical Society*, vol. 24, no. 3, pp. 334–344, 2020.

[9] G. Seilkhanova, A. Imangaliyeva, Y. Mastai, and A. Rakhym, "Bentonite polymer composite for water purification," *Bulletin of Materials Science*, vol. 42, no. 60, pp. 1–8, 2019.

[10] Syafalni, R. Abdullah, I. Abustan, and A. Ibrahim, Wastewater treatment using bentonite, the combinations of bentonite-zeolite, bentonite-alum, and bentonite-limestone as adsorbent and coagulant," *International Journal of Environmental Sciences*, vol. 4, no. 3, pp. 379–391, 2013.

[11] K. Noufel, N. Djebri, N. Boukhalfa, M. Boutahala, and A. Dakhouche, "Removal of bisphenol A and trichlorophenol from aqueous solutions by adsorption with organically modified bentonite, activated carbon composites: a comparative study in single and binary systems," *Groundwater for Sustainable Development*, vol. 11, pp. 1–11, 2020.

[12] V. Rizzi, J. Gubitosa, P. Fini et al., "Chitosan film as recyclable adsorbent membrane to remove/recover hazardous pharmaceutical pollutants from water: the case of the emerging pollutant Furosemide," *Journal of Environmental Science and Health, Part A*, vol. 602, no. 5, pp. 1–12, 2020.

[13] D. Ewis, A. Benamor, M. M. Ba-Abbad, M. Nasser, M. El-Naas, and H. Qiblawey, "Removal of oil content from oil-water emulsions using iron oxide/bentonite nano adsorbents," *Journal of Water Process Engineering*, vol. 38, pp. 1–11, 2020.

[14] C. Yu, J. Shao, W. Sun, and X. Yu, "Treatment of lead contaminated water using synthesized nano-iron supported with bentonite/graphene oxide," *Arabian Journal of Chemistry*, vol. 13, no. 1, pp. 3474–3483, 2020.

[15] R. R. Pawar and Lalhmunsiama, P. G. Ingole and S.-M. Lee, Use of activated bentonite-alginate composite beads for efficient removal of toxic $Cu^{2+}$ and $Pb^{2+}$ ions from aquatic environment," *International Journal of Biological Macromolecules*, vol. 164, pp. 3145–3154, 2020.

[16] Z. Wang, G. Chen, X. Wang, S. Li, Y. Liu, and G. Yang, "Removal of hexavalent chromium by bentonite supported organosolv lignin-stabilized zero-valent iron nanoparticles from wastewater," *Journal of Cleaner Production*, vol. 267, pp. 1–11, 2020.

[17] V. Masindi and M. M. Ramakokovhu, "The performance of thermally activated and vibratory ball milled South African bentonite clay for the removal of chromium ions from aqueous solution," *Materials Today: Proceedings*, vol. 38, pp. 1–11. In press, 2020.

[18] B. Thakur, G. Sharma, A. Kumar et al., "Designing of bentonite based nanocomposite hydrogel for the adsorptive removal and controlled release of ampicillin," *Journal of Molecular Liquids*, vol. 319, pp. 1–14, 2020.

[19] F. Dardir, A. Mohamed, M. Abukhadra, E. Ahmed, and M. Soliman, "Cosmetic and pharmaceutical qualifications of

Egyptian bentonite and its suitability as drug carrier for Praziquantel drug," *European Journal of Pharmaceutical Sciences*, vol. 115, pp. 320–329, 2018.

[20] C. Santi, S. Cortes, L. D'Acqui, E. Sparvoli, and B. Pushparaj, "Reduction of organic pollutants in olive mill wastewater by using different mineral substrates as adsorbents," *Bioresource Technology*, vol. 99, no. 6, pp. 1945–1951, 2008.

[21] M. Mahasneh and K. Shakhatreh, "Evaluation of Jordanian bentonite performance for drilling fluid applications," *Contemporary Engineering Sciences*, vol. 5, no. 3, pp. 149–170, 2012.

[22] R. Al Dwairi and A. Al-Rawajfeh, "Removal of cobalt and nickel from wastewater by using Jordan low-cost zeolite and bentonite," *Journal of the University of Chemical Technology and Metallurgy*, vol. 47, no. 1, pp. 69–76, 2012.

[23] F. Khalili, N. Salameh, and M. Shaybe, "Sorption of uranium(vi) and thorium(iv) by Jordanian bentonite," *Journal of Chemistry*, vol. 2013, Article ID 586136, 13 pages, 2013.

[24] I. Hamadneh, R. Abu-Zurayk, B. Abu-Irmaileh, A. Bozeya, and A. Al-Dujaili, "Adsorption of pb(II) on raw and organically modified Jordanian bentonite," *Clay Minerals*, vol. 50, pp. 485–496, 2015.

[25] P. Huong, B. Lee, K. Jitae, and C. Lee, "Nitrophenols removal from aqueous medium using Fe-nano mesoporous zeolite," *Materials & Design*, vol. 101, pp. 210–217, 2016.

[26] F. Cermola, M. Dellagreca, R. Iesce, S. Montella, A. Pollio, and F. Temussi, "A mild photochemical approach to the degradation of phenols from olive oil mill wastewater," *Chemosphere*, vol. 55, pp. 1035–1041, 2004.

[27] I. Maulana and F. Takahashi, "Cyanide removal study by raw and iron-modified synthetic zeolites in bath adsorption experiment," *Journal of Water Process Engineering*, vol. 22, pp. 80–86, 2018.

[28] H. Polat, M. Molva, and M. Polat, "Capacity and mechanism of phenol adsorption on lignite," *International Journal of Mineral Processing*, vol. 79, no. 4, pp. 264–273, 2006.

[29] C. Mahugo-Santana, Z. Sosa Ferrera, E. M. Torres Padrón, and J. J. Santana Rodríguez, "Methodologies for the extraction of phenolic compounds from environmental samples: new approaches," *Molecules*, vol. 14, no. 1, pp. 298–320, 2009.

[30] P. Huong, B. Lee, K. Jitae, and C. Lee, "Improved removal of 2-chlorophenol by a synthesized Cu-nano zeolite," *Process Safety and Environmental Protection*, vol. 100, pp. 272–280, 2016.

[31] L. Zhao, J. Ma, Z. Sun, and X. Zhai, "Mechanism of influence of initial pH on the degradation of nitrobenzene in aqueous solution by ceramic honeycomb catalytic zonation," *Environmental Science & Technology*, vol. 42, no. 11, pp. 4002–4007, 2008.

[32] P. Huong, B. Lee, K. Jitae, and C. Lee, "Improved adsorption properties of a nanozeolite adsorbent toward toxic nitrophenols," *Process Safety and Environmental Protection*, vol. 104, pp. 314–322, 2016.

[33] G. Yang, H. Chen, H. Qin, and Y. Feng, "Amination of activated carbon for enhancing phenol adsorption: effect of nitrogen-containing functional groups," *Applied Surface Science*, vol. 293, pp. 299–305, 2014.

[34] E. Escrich, R. Moral, and M. Solanas, "Olive oil, an essential component of the mediterranean diet, and breast cancer," *Public Health Nutrition*, vol. 14, no. 12A, pp. 2323–2332, 2011.

[35] A. Khdair and G. Abu-Rumman, "Sustainable environmental management and valorization options for olive mill byproducts in the middle east and north Africa (MENA) region," *Processes*, vol. 8, no. 671, pp. 1–22, 2020.

[36] P. Paraskeva and E. Diamadopoulos, "Technologies for olive mill wastewater (OMW) treatment: a review," *Journal of Chemical Technology and Biotechnology*, vol. 81, pp. 1475–1485, 2006.

[37] I. Leouifoudi, A. Zyad, A. Amechrouq, M. Oukerrou, H. Mouse, and M. Mbarki, "Identification and characterisation of phenolic compounds extracted from Moroccan olive mill wastewater," *Food Science and Technology*, vol. 34, no. 2, pp. 249–257, 2014.

[38] S. M. Seyed Arabi, R. S. Lalehloo, M. R. T. B. Olyai, G. A. M. Ali, and H. Sadegh, "Removal of Congo red azo dye from aqueous solution by ZnO nanoparticles loaded on multiwall carbon nanotubes," *Physica E: Low-Dimensional Systems and Nanostructures*, vol. 106, pp. 150–155, 2019.

[39] H. Abdel Ghafar, G. A. M. Ali, O. Fouad, and S. Makhlouf, "Enhancement of adsorption efficiency of methylene blue on Co3O4/SiO2 nanocomposite," *Desalination and Water Treatment*, vol. 53, no. 11, pp. 2980–2989, 2015.

[40] J. Madejová, J. Kečkéš, H. Pálková, and P. Komadel, "Identification of components in smectite/kaolinite mixtures," *Clay Minerals*, vol. 37, no. 2, pp. 377–388, 2002.

[41] W. Mekhamer, "Energy storage through adsorption and desorption of water vapour in raw Saudi bentonite," *Arabian Journal of Chemistry*, vol. 9, pp. S264–S268, 2016.

[42] L. Zhirong, M. Azhar Uddin, and S. Zhanxue, "FT-IR and XRD analysis of natural Na-bentonite and Cu(II)-loaded Na-bentonite," *Spectrochimica Acta Part A: Molecular and Biomolecular Spectroscopy*, vol. 79, no. 5, pp. 101–1016, 2011.

[43] A. Tabak, B. Afsin, B. Caglar, and E. Koksal, "Characterization and pillaring of a Turkish bentonite (resadiye)," *Journal of Colloid and Interface Science*, vol. 313, no. 1, pp. 5–11, 2007.

[44] R. Ajemba, "Structural alteration of bentonite from nkaliki by acid treatment: studies of the kinetics and properties of the modified samples," *International Journal of Advances in Engineering & Technology*, vol. 7, no. 1, pp. 379–392, 2014.

[45] D. Manohar, B. Noeline, and T. Anirudhan, "Adsorption performance of Al-pillared bentonite clay for the removal of cobalt(II) from aqueous phase," *Applied Clay Science*, vol. 31, no. 3-4, pp. 194–206, 2006.

[46] M. Naswir, S. Arita, M. Marsi, and S. Salni, "Characterization of bentonite by XRD and SEM-EDS and use to increase pH and color removal, Fe and organic substances in peat water," *Journal of Clean Energy Technologies*, vol. 1, no. 4, pp. 313–317, 2013.

[47] G. Batdemberel, T. Battumur, T. S. Enkhtuya, G. Tsermaa, and S. Chadraabal, ""Synthesis of ZnO nanoparticles by mechanochemical processing," in *Proceedings of the 4th International Conference on X-ray Analysis*, vol. 1, pp. 47-48, Ulaanbaatar, Mongolia, June 2015.

[48] K. Margeta, N. Logar, M. Šiljeg, and A. Farkas, "Water treatment," in *Chapter 5 (Natural Zeolites in Water Treatment—How Effective is Their Use)*, W. Elshorbagy and R. K. Chowdhury, Eds., pp. 81–111, IntechOpen, London, UK, NV, USA, 2013, https://www.intechopen.com/books/water-treatment/natural-zeolites-in-water-treatment-how-effective-is-their-use?jwsource=cl&ref=driverlayer.com.

[49] Y. Huang, Y. Zhang, G. Han et al., "Sodium-modification of Ca-based bentonite via semidry process," *Journal of Central South University of Technology*, vol. 17, no. 6, pp. 1201–1206, 2010.

[50] R. Sheikh, *The synthesis of cementitious compounds in molten salts*, Phd Thesis, Department of Chemical Engineering University College, London, UK, 2016.

[51] K. Akpomie, F. Dawodu, and K. Adebowale, "Mechanism on the sorption of heavy metals from binary-solution by a low cost montmorillonite and its desorption potential," *Alexandria Engineering Journal*, vol. 54, pp. 757–767, 2015.

[52] M. Elmashad, "Effect of chemical additives on consistency, infiltration rate and swelling characteristics of bentonite," *Water Science*, vol. 31, pp. 177–188, 2017.

[53] T. Schanz and S. Tripathy, "Swelling pressure of a divalent-rich bentonite: diffuse double-layer theory revisited," *Water Resources Research*, vol. 45, pp. 1–9, 2009.

[54] C. I. Piperidou, C. I. Chaidou, C. D. Stalikas, K. Soulti, G. A. Pilidis, and C. Balis, "Bioremediation of olive oil mill wastewater: chemical alterations induced byazotobactervinelandii," *Journal of Agricultural and Food Chemistry*, vol. 48, no. 5, pp. 1941–1948, 2000.

[55] E. Eroglu, I. Eroglu, U. Gündüz, and M. Yücel, "Effect of clay pretreatment on photofermentative hydrogen production from olive mill wastewater," *Bioresource Technology*, vol. 99, pp. 6799–6808, 2008.

[56] F. Hanafi, N. Sadif, O. Assobhei, and M. Mountadar, "Traitement des margines par électrocoagulation avec des électrodes plates en aluminium," *Journal of Water Science*, vol. 22, no. 4, pp. 473–485, 2009.

[57] E. Moreno, J. Pérez, A. Ramos-Cormenzana, and J. Martínez, "Antimicrobial effect of waste water from olive oil extraction plants selecting soil bacteria after incubation with diluted waste," *Microbios*, vol. 51, pp. 169–174, 1987.

[58] A. Vlyssides, M. Loizides, and P. Karlis, "Integrated strategic approach for reusing olive oil extraction by-products," *Journal of Cleaner Production*, vol. 12, no. 6, pp. 603–611, 2004.

[59] M. Mouncif, S. Tamoh, M. Faid, and A. Achkari-Begdouri, "A study of chemical and microbiological characteristics of olive mill waste water in Morocco," *Grasas Y Aceites*, vol. 44, pp. 335–338, 1993.

[60] D. Bouknana, B. Hammouti, R. Salghi et al., "Physicochemical characterization of olive oil mill wastewaters in the eastern region of Morocco," *Journal of Materials and Environmental Science*, vol. 5, no. 4, pp. 1039–1058, 2014.

[61] A. Aly, Y. Hasan, and A. Al-Farraj, "Olive mill wastewater treatment using a simple zeolite-based low-cost method," *Journal of Environmental Management*, vol. 145, pp. 341–348, 2014.

[62] M. Panizza and G. Cerisola, "Olive mill wastewater treatment by anodic oxidation with parallel plate electrodes," *Water Research*, vol. 40, pp. 1179–1184, 2006.

[63] J. Alba, "Nuevas tecnologías para la obtención del aceite de olive," *Fruticultura Profesional (Suplemento)*, vol. 62, pp. 85–95, 1994.

[64] P. Passarinho, *Olive Mill Wastewater Detoxification*, Ph.D Thesis, Instituto Superior Técnico, Universidade Técnica de Lisboa, Lisbon, Portugal, 2002.

[65] M. Hamdi, "Thermoacidic precipitation of darkly coloured polyphenols of olive mill wastewaters," *Environmental Technology*, vol. 14, pp. 495–500, 1993.

[66] R. Kant and M. Singh, "Generalization of linearized gouy-chapman-stern model of electric double layer for nano-structured and porous electrodes: deterministic and stochastic morphology," *Physical Review E*, vol. 88, no. 5, pp. 1–36, 2013.

[67] M. Setz, K. Tian, C. Benson, and S. Bradshaw, "Effect of ammonium on the hydraulic conductivity of geosynthetic clay liners," *Geotextiles and Geomembranes*, vol. 45, pp. 665–673, 2017.

[68] J. Frankovská, S. Andrejkovičová, and I. Janotka, "Effect of NaCl on hydraulic properties of bentonite and bentonite-palygorskite mixture," *Geosynthetics International*, vol. 17, no. 4, pp. 250–259, 2010.

[69] L. G. Wade, *Phenol*, Encyclopaedia Britannica, Inc., Chicago, IL, USA, 2018.

[70] H. Sadegh, G. A. M. Ali, S. Agarwal, and V. K. Gupta, "Surface modification of MWCNTs with carboxylic-to-amine and their superb adsorption performance," *International Journal of Environmental Research*, vol. 13, no. 3, pp. 523–531, 2019.

[71] J. Acharya, J. N. Sahu, C. R. Mohanty, and B. C. Meikap, "Removal of lead(II) from wastewater by activated carbon developed from Tamarind wood by zinc chloride activation," *Chemical Engineering Journal*, vol. 149, no. 1-3, pp. 249–262, 2009.

[72] R. Ocampo-Perez, R. Leyva-Ramos, J. Mendoza-Barron, and R. Guerrero-Coronado, "Adsorption rate of phenol from aqueous solution onto organobentonite: surface diffusion and kinetic models," *Journal of Colloid and Interface Science*, vol. 364, pp. 195–204, 2011.

[73] M. Akl, M. Dawy, and A. Serage, "Efficient removal of phenol from water samples using sugarcane bagasse based activated carbon," *Journal of Analytical & Bioanalytical Techniques*, vol. 5, no. 2, pp. 1–12, 2014.

[74] H. Bradl, "Adsorption of heavy metal ions on soils and soils constituents," *Journal of Colloid and Interface Science*, vol. 277, no. 1, pp. 1–18, 2004.

[75] V. Gupta, S. Agarwal, H. Sadegh, G. A. M. Ali, A. K. Bharti, and A. S. Hamdy, "Facile route synthesis of novel graphene oxide-$\beta$-cyclodextrin nanocomposite and its application as adsorbent for removal of toxic bisphenol A from the aqueous phase," *Journal of Molecular Liquids*, vol. 237, pp. 466–472, 2017.

[76] A. Taiwo and N. Chinyere, "Sorption characteristics for multiple adsorption of heavy metal ions using activated carbon from nigerian bamboo," *Journal of Materials Science and Chemical Engineering*, vol. 4, no. 4, pp. 39–48, 2016.

[77] N. Ahalya, R. Kanamadi, and T. Ramachandra, "Biosorption of chromium (VI) from aqueous solutions by the husk of Bengal gram (Cicer arientinum)," *Electronic Journal of Biotechnology*, vol. 8, no. 3, pp. 258–264, 2005.

[78] H. Boparai, M. Joseph, and D. O'Carroll, "Kinetics and thermodynamics of cadmium ion removal by adsorption onto nano zerovalent iron particles," *Journal of Hazardous Materials*, vol. 186, pp. 458–465, 2011.

[79] A. Inyinbor, F. Adekola, and G. Olatunji, "Kinetics, isotherms and thermodynamic modeling of liquid phase adsorption of rhodamine B dye onto raphia hookerie fruit epicarp," *Water Resources and Industry*, vol. 15, pp. 14–27, 2016.

[80] A. Turco and C. Malitesta, "Removal of phenolic compounds from olive mill wastewater by a polydimethylsiloxane/oxMWCNTs porous nanocomposite," *Water*, vol. 12, pp. 1–13, 2020.

[81] A. S. Stasinakis, I. Elia, A. V. Petalas, and C. P. Halvadakis, "Removal of total phenols from olive-mill wastewaterusing an agricultural by-product, olive pomace," *Journal of Hazardous Materials*, vol. 160, no. 2-3, pp. 408–413, 2008.

[82] A. De Martino, M. Iorio, P. D. Prenzler, D. Ryan, H. K. Obied, and M. Arienzo, "Adsorption of phenols from olive oil waste waters on layered double hydroxide, hydroxyaluminium-iron-co-precipitate and hydroxyaluminium-iron-montmorillonite complex," *Applied Clay Science*, vol. 80-81, pp. 154–161, 2013.

[83] S. I. Mustapha, F. A. Aderibigbe, T. L. Adewoye, I. A. Mohammed, and T. O. Odey, "Silver and titanium oxides for the removal of phenols from pharmaceutical wastewater," *Materials Today: Proceedings*, vol. 38, pp. 2–7, 2020.

[84] E. M. Silva, D. R. Pompeu, Y. Larondelle, and H. Rogez, "Optimisation of the adsorption of polyphenols from inga edulis leaves on macroporous resins using an experimental design methodology," *Separation and Purification Technology*, vol. 53, pp. 274–280, 2007.

[85] D. Pinelli, A. E. M. Bacca, A. Kaushik et al., "Batch and continuous flow adsorption of phenolic compounds from olive mill wastewater: a comparison between nonionic and ion exchange resins," *International Journal of Chemical Engineering*, vol. 2016, Article ID 9349627, 13 pages, 2016.

[86] M. L. Soto, A. Moure, H. Domínguez, and J. C. Parajó, "Batch and fixed bed column studies on phenolic adsorption from wine vinasses by polymeric resins," *Journal of Food Engineering*, vol. 209, pp. 52–60, 2017.

[87] I. A. W. Tan, J. C. Chan, B. H. Hameed, and L. L. P. Lim, "Adsorption behavior of cadmium ions onto phosphoricacid-impregnated microwave-induced mesoporous activated carbon," *Journal of Water Process Engineering*, vol. 14, pp. 60–70, 2016.

[88] D. Ghahremani, I. Mobasherpour, and S. Mirhosseini, "Sorption thermodynamic and kinetic studies of Lead removal from aqueous solutions by nano tricalcium phosphate," *Bulletin de la Société Royale des sciences de Liège*, vol. 86, pp. 96–112, 2017.

[89] K. G. Bhattacharyya and S. S. Gupta, "Kaolinite, montmorillonite, and their modified derivatives as adsorbents for removal of Cu(II) from aqueous solution," *Separation and Purification Technology*, vol. 50, no. 3, pp. 388–397, 2006.

[90] Q. Zhao, H. Choo, A. Bhatt, S. Burns, and B. Bate, "Review of the fundamental geochemical and physical behaviors of organoclays in barrier applications," *Applied Clay Science*, vol. 142, pp. 2–20, 2017.

[91] N. Selçuk, Ş. Kubilay, A. Savran, and A. Kul, "Kinetics and thermodynamic studies of adsorption of methylene blue from aqueous solutions onto Paliurus spina-christi mill. Frutis and seeds," *IOSR Journal of Applied Chemistry*, vol. 10, no. 5, pp. 53–63, 2017.

[92] N. Mubarak, A. Jawad, and W. Nawawi, "Equilibrium, kinetic and thermodynamic studies of reactive red 120 dye adsorption by chitosan beads from aqueous solution," *Energy, Ecology and Environment*, vol. 2, no. 1, pp. 85–93, 2017.

[93] S. Al-Jubouri and S. Holmes, "Hierarchically porous zeolite X composites for manganese ion-exchange and solidification: equilibrium isotherms, kinetic and thermodynamic studies," *Chemical Engineering Journal*, vol. 308, pp. 476–491, 2017.

[94] K. Akpomie and F. Dawodu, "Potential of a low-cost bentonite for heavy metal abstraction from binary component system," *Beni-Suef University Journal of Basic and Applied Sciences*, vol. 4, pp. 1–13, 2015.

[95] A. Witek-Krowiak, "Application of beech sawdust for removal of heavy metals from water: biosorption and desorption studies," *European Journal of Wood and Wood Products*, vol. 71, no. 2, pp. 227–236, 2013.

[96] M. J. Lashaki, M. Fayaz, H. Wang et al., "Effect of adsorption and regeneration temperature on irreversible adsorption of organic vapors on beaded activated carbon," *Environmental Science Technology*, vol. 46, pp. 4083–4090, 2012.

[97] S. E. Abechi, "Studies on the mechanism of adsorption of methylene blue onto activated carbon using thermodynamic tools," *Science World Journal*, vol. 13, no. 2, pp. 17–19, 2018.